SSRG International Journal of Mechanical Engineering
ISSN: 2348-8360/ https://doi.org/10.14445/23488360/IJME-V13I7P122

Volume 13 Issue 7, 281-296, July 2026


*Original Article*

# Friction Stir Lap Welding of Al 6061-T6 using Bobbin Tool Designed for Lapped Workpieces

Vijaykumar Natvarlal Modi[1, 2], Anishkumar H. Gandhi[3*], Vishvesh J. Badheka[4], Kishan Fuse[4]

[1]*Gujarat Technological University, Gujarat, India.*
[2]*Department of Mechanical Engineering, Government Engineering College, Gandhinagar, Gujarat, India.*
[3]*IPsecuR Services, Surat, Gujarat, India.*
[4]*Department of Mechanical Engineering, School of Technology, Pandit Deendayal Energy University, Gandhinagar, India.*

[3*]*Corresponding Author : anishgandhi2002@yahoo.co.in*

Received: 27 May2026 Revised: 23 June 2026 Accepted: 04 July 2026 Published: 30 July 2026

***Abstract*** *- Al 6061 has been shown to be a viable candidate material for structural light weighting of transportation vehicles due to its exceptional extrudability, high strength with low weight, and excellent resistance to corrosion. Friction Stir Welding (FSW) has proved its cutting edge for the Aluminum structure assembly in transportation industries due to less heat involvement in the process, mitigates solidification cracking and improves mechanical performance in the assembly. In present study, newly designed bobbin tool was used to investigate weld quality of plates (152 X 102 X 3) mm of Al 6061-T6 in lapped configuration. A bobbin tool with 3 different profiles parts in a pin and concave shoulders was used to investigate effect of different tool rotation (w) speeds- 280, 350 and 445 RPM on Mechanical properties and micro structure of lap joint. Experiments were performed with fixed welding travel speed (v) of 16 mm/min and with conductive heat flow restriction mode. Weld quality was checked with visual inspection, macrostructure, microstructure, tensile-shear strength and hardness. Results showed that newly designed tool is capable to generate strong vertical and horizontal material flow and inter mixing of top and bottom plates materials. All weld samples were fractured from advancing side of bottom plate in tensile-shear test. Maximum Ultimate Tensile Strength (UTS) value and maximum microhardness value was reported as 136.98 $N/mm^2$ and 56.6 HV respectively at tool rotational speed 445 RPM.*

***Keywords*** *- Lap Welding, Aluminum alloy, Treaded Pin, Microstructure, Mechanical properties, Hooks, Cold lap.*

## 1. Introduction

High-strength and lightweight materials and structures are in high demand due to its various applications, such as ground transportation, aviation, military and aerospace applications [1]. Lightweight alloys play a major role in such applications, and it's crucial to weld such materials efficiently.

From invention of Friction Stir Welding (FSW) [2] to its advanced modifications, it's played an effective role for the welding of same kind and/or different kind of materials including Alluminum and its alloys, copper and copper alloy [3], Steel [4, 5] Magnesium alloys [6, 7], Titanium [4, 8, 9], [10, 11] and composites of metals [12-14] and even wood-plastics [15] also, in various configurations as butt, lap, corner, and fillet.

The Conventional Tool Friction Stir Welding (CTFSW) is successfully and widely applied due to its many benefits and "green nature" [16], but has some limitations or drawbacks. Void or tunnel or pore or wormhole defects, root defects, need of back plate, heat leakage issue due to a back plate, fixture to control z force, these are in the list of issues with FSW. TWI developed a new variant named as Bobbin Tool Friction Stir Welding (BTFSW) [17] to limit or overcome the defects produced in CTFSW has number of advantages such as elimination of root defects, under welding defects, weld roots, no need of back plate and low Z forces due to its top and bottom shoulders is called double sided friction stir tool or self- reacting friction stir welding tool. Uniform heat distribution and a roughly rectangle nugget zone are the characteristics of BTFSW due to the top and bottom solders of the bobbin tools.

Additionally, one more advantage of BTFSW is that the workpieces ideally experience net zero Z forces, which results in machine design and, in turn, reduces machine cost [18].

In FSW, the shoulder and pin's spinning speeds stir the workpiece materials. Figure 1 (a), and (b) illustrates the material stirs at the shoulders, the material interface, and the pin interface. A horizontal flow of material is produced by tool feed. Shoulder pressure and tool design result in little vertical material flow. Due to the vertical base material separation surface in the butt configuration, this inadequate material flow is less of an issue than it is in the lap configuration, which has a horizontal base material separation interface.

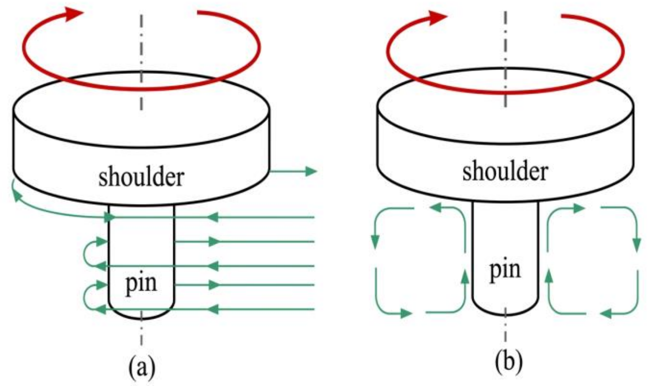


**Fig. 1 Material flow in FSW, (a) in horizontal direction, (b) in vertical direction [5].**

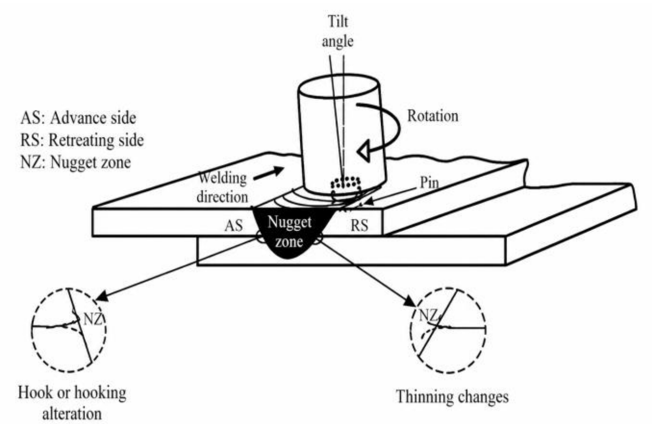


**Fig. 2 Schematic friction stir lap welding and hooks and plate thinning geometries [22]**

FSW of lapped workpieces is more tricky than in butted workpieces because of the horizontal workpiece separation surfaces and horizontal material flow in the lap configuration, which requires both vertical and horizontal material flow, whereas in the butt configuration, vertical workpiece separation surfaces and horizontal material flow are also required [19-21].

Due to the horizontal interface in lap welding as opposed to the vertical interface in butt welding, a distinctive feature of the occurrence of crack-like unbonded at the mating surface of workpieces is inevitable is termed as hooking effect on AS and termed as cold lap at RS of the weld [22], and responsible for generation of plate thinning or plate thickening in welded lapped workpieces which is shown in Figure 2.

These adverse characteristics propagate shear stress during tensile testing of welded workpieces due to reduced cross-section and provide a solid reason for a large reduction in tensile-shear strength of welded lapped workpieces compared to the base material.

Other issues with the FSLW is termed joint line defect or ROD or joint line remnant or kissing bond [1], wormhole or tunnel, void. Oxide layers on the bottom surface of the top plate and top surface of the bottom plates traps in between two mating surfaces in lap welding creates Residual Oxide Defects (ROD). These characteristics play a role as a stress booster and majorly accountable for the lap joints' failure [9, 18, 19, 23, 24].

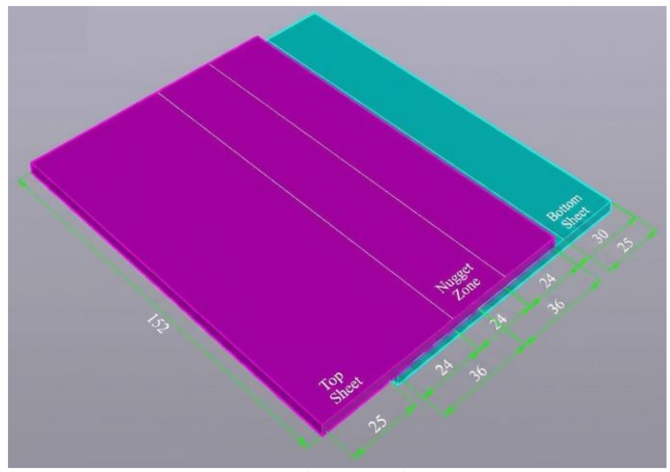


**Fig. 3 Sheet layout configuration for experiment [25]**

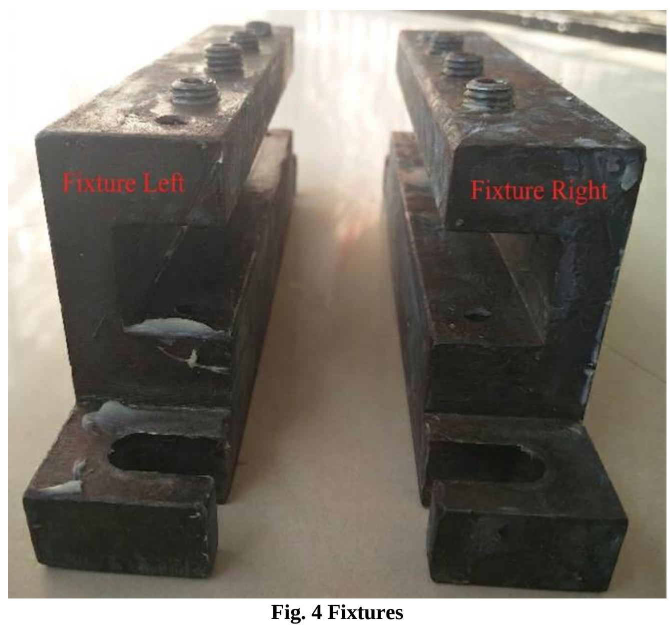


**Fig. 4 Fixtures**

The friction stir welding technique has attracted a lot of attention, and a significant amount of work has been done using CTFSW for the lap joint of Aluminum alloys and composites. Optimizing the welding performance of FSW requires a significant amount of work.

**Table 1. Summarized literature review of BTFSLW, CTFSBW, and CTFSLW**

| Sr. | Workpiece Details | Tool Details | Experimental Details | Outcomes/Conclusions | Ref |
|---|---|---|---|---|---|
| 1 | AA 1050 H14, thickness 10 mm | BT, H13 tool steel; Shoulders: Ø 25 mm, 6° concave; Pin: (cylinder, triangular, square) cross section, Øinside 10 mm, flat; Shoulder gap: 5 mm | BTFSLW; w 600 rpm; v (200 - 400-600) mm/min; optimization: Tw, TSL and hardness | Travel speed greatly influenced TLS and Tw; Tool shape influenced hardness; Minimum temperature generated with triangular pin geometry at 600 mm/min. | [26] |
| 2 | AA 1050 H14, thickness 10 mm | BT, H13 tool steel; Shoulders: Ø 25 mm, 6° concave; Pin: (cylinder, triangular, square) cross section, Øinside 10 mm, flat; Shoulder gap: 5 mm | BTFSLW; w 600 rpm; v (200-400-600-1000) mm/min; Study: Temperatures at weld centre line, AS and RS; microstructure, tensile property, hardness, surface fracture | Highest stir zone temperature 380° by square pin at travel speed 200 mm/min; Lowest stir zone temperature by triangular pin; Temperature α 1/w; Temperature at AS was 20° higher than RS; Highest UTS by square pin at travel speed 200 mm/min and 600 mm/min; Triangular pin produced joint with defects; Mixed brittle-ductile fracture observed. | [27] |
| 3 | AA 6061-T6 (200 X 150 mm X 4) mm | CT, H13 tool steel (hot worked); Shoulder: Ø 17 mm, concave; Pin: conical, Ømax 6 mm, Ømin 4 mm, L 5 mm | CTFSLW; 5 pass overlapped (0%, 25%, 50%, 75%); Tool tilt 1.5°; Tool plunge 0.2 mm | Defects reduced at higher overlapping; 75% overlapping resulted in zero defect; UTSmax value of 230 MPa at 50% overlap and UTSmin value of 160 MPa at 0% overlap; Kissing bond formation at 75% overlap; All samples broke towards RS; Brittle; ductile and mixed mode failure observed; microhardness values ranging from 43 $HV_{0.1}$ to 49 $HV_{0.1}$; With high overlapping%, little higher microhardness values were observed. | [21] |
| 4 | Al 6061, thickness (2 and 5) mm; graphene Nano platelets (GNPs) at the weld interface (100 X 75 X 5) mm, Overlap 40 mm, | CT, H13 tool steel (hot worked); Shoulder: cylindrical, Ø 18 mm, flat; Pin: square (6 x 6) mm, L 3 mm | CTFSLW; w 1400 rpm; v 40 mm/min, Tool tilt 2°, Tool plunge 0.2 mm | 121% increment in weld strength and 53% increments in elongation due to GNPs; The hook height decreased by 26%, and the cold lap height decreased by 41%; Formation of the $Al_2O_3$ layer was reduced by the GNP interlayer; the grain size reduced to ~ 5.18 to ~ 8.37 µm from the ~ 22 µm. | [12] |
| 5 | Top plate-Al 6061-T6 (T 3 mm), Ultra low carbon steel (T 0.8 mm) | CT, Coated WC-CO tool; Shoulder: cylindrical, Ø 20 mm, flat; Pin: cylindrical, Ø 5 mm, flat; L 3 mm | Dissimilar CTFSLW; w 1200 rpm; v (60-100-140-200) mm/min; 0.2 mm tool offset (in steel); Tool tilt 5°; Tool pin plunge 0.2 mm in bottom steel plate | UTS value increased up to maximum (tensile load of 3.6 KN) as v increased up 200 mm/min; UTS was associated with the intermetallic reactions at the joint interface in nearby 1 µm; As v increased, TMAZ and HAZ size decreased. | [28] |
| 6 | Top plate-AA6061 (200 X 70 X 3) mm, | CT, W-25Re alloy tool; Shoulder: cylindrical, Ø 12 | Dissimilar CTFSLW; w (800-1000-1200) rpm; v (50-100-200-300-400) mm/min; | No hooking; Tensile failure along the interface; Increased heat input resulted in interface thickness increment; $TiAl_3$ was the major component in intermetallic | [29] |

| | | | | | |
|---|---|---|---|---|---|
| | Ti6Al4V (200 X 70 X 2) mm | mm, concave; Pin: conical Ømax 3 mm, flat, L 3.1 mm | tool tilt 3°; Tool plunge 0.1 mm | compound; UTS increased with increased interface thickness, initially at 7.5-µm-thick interface, shear load value was 4500 N (maximum) at w 1000 rpm and v 100 mm/min, and then found in negative manner; Micro cracks at IMC resulted in failure of weldments; Excessive IMC formation at higher interface thickness. | |
| 7 | Al 6061-T6 (300 X 300 X 3) mm | CT, H13 tool steel (hot worked); Shoulder: cylindrical, Ø 18 mm, flat; Pin: cylindrical, Ø 6 mm, flat, L 5 mm | Dissimilar CTFSLW; w (800, 1000, 1200) rpm; v (30, 45, 60) mm/min; Axial load (9.5, 11, 12.5) kN | w had the maximum 51%, v had 38%, and the axial load had 8% contribution in shear strength; UTS found 60 MPa at load (axial) 11.5 kN, w 1200 rpm and v 45 mm/min | [20] |
| 8 | Al 6061-T6 (150 X 80 X 1) mm | CT, Hot worked abrasives steel Shoulder: cylindrical, Ø 7 mm, flat; Pin: (quadrangular frustum pyramid-Smax 2 mm, Smin-1.5 mm); (conical-Ømax 2 mm, Ømin 1.5 mm); (square-2 X 2 mm), flat, L 0.9 mm | CT High speed FSBW; w 11000 rpm; v (200, 300, 400, 500) mm/min; Used high rotation speed FSW machine | UTS was 87.2% (265 MPa) of BM at w 11000 rpm and v 300 mm/min; Low angle boundaries were lower than that of traditional FSBW; "Flat T" pattern was observed in the joint; Equiaxed grains with grain Øavg was 9.3 µm observed in NZ. | [30] |
| 9 | Al 6061-T6 (300 X 140 X 3) mm; Overlap 50 mm | CT, H13 tool steel (hot worked); Shoulder: cylindrical, Øout 15 mm, Øinr 5.2 mm, concave flat; Pin: conical, Ømax 4.5 mm, Ømin 3.5 mm, L 4 mm, RH threaded with pitch 0.8 mm. | Stationary shoulder FSLW; w (1000, 1200, 1400, 1600) rpm; v 50 mm/min; Tool tilt 2.5°; Tool plunge 0.2 mm | No shoulder marks; Bowl-like cross-section morphology; Max shear load max 17.01 kN at w 1200 rpm; Max. EST at 1200 rpm; Max. ELW at 1600 rpm; Initially, shear load increased with increase in rotational speed and decreased later on; Ductile failure; Shear and tensile failure observed. | [31] |
| 10 | Al 6061-T6, T 2.5 mm, polyether ether ketone (PEEK) T 7 mm | CT; Shoulder: Ø 14 mm, concave; Pin: tapered thread, triple facets, L 4.8 mm | Dissimilar CTFSLW; w 900 rpm; v (30-50-70-90) mm/min; Tool tilt 2.0°; Tool plunge 0.2 mm | Sound joint formation due to elongated, deformed and bended Al anchor interlocking mechanically and penetrated into polymer (molten and again re-solidified); Anchor size and gap width at the interface were reduced due to decreased heat input. | [32] |
| 11 | Base plate-AISI 1018 CS, T 6.35 mm; Cladding plate-AISI 316L SS, T 2.7 mm, cold rolled, annealed. | CT, PCBN; Shoulder: Ø 24 mm; Pin: Ø 7.6 mm, L 3.7 mm | Dissimilar CTFSLW; v (20-30) ipm | Refined microstructure; Recrystallized austenitic grains (3 µm grain size); Refinement of grain size from 8 µm to 2 µm; Microhardness was 250 HV and 200 HV on the SS plate and the CS plate, respectively. Maximum load carrying capacity was 7 kN; the UTS of the weld was 600 MPa, which was 100 MPa higher than the BM. For the clad, the passive range of corrosion potential was 500 mV. | [33] |

| | | | | | |
|---|---|---|---|---|---|
| | | | | Electrochemical properties of the weld and the BM were found to be similar. | |
| 12 | Sheet 1- CRFTP (PA6 with carbon fiber 20 wt.%), T 3 mm;<br>Sheet 2- Copper ($O_2$ free), T 2 mm; carbon fiber- (Ø 10 X L 500) mm; Overlap 30 mm | CT, Tool steel; Shoulder: Ø 15 mm; Pin: No | CTFSLW;<br>w 1500 rpm; v (1200–1600) mm/min; Tool tilt 3°; Tool plunge 0.9 mm | Hydrogen bonding formed on the Cu surface contributed largely in lap joint weld due to the bonding formation of copper oxide and CFRTP amid group; Initially TSF increased up to 2.3 kN and decreased later on with the joining speed increment; | [34] |
| 13 | Review article | Review article | Review article | Brittle IMC formation due to peak temperature; Weak joint (brittle) formation due to thick layer of intermetallic; Control of the intermetallic thickness is difficult; Application of bigger pin Ø and low w can produce strong weld joint forming little amount of IMC; Formation of IMC can be reduced by controlling peak temperature using some cooling mediums; Elimination of brittle IMC formation can be done by application of Zn as filler layer. | [3] |
| 14 | Top plate- AA7075 (100 X 200 X 3) mm,<br>Bottom plate- (100 X 200 X 5) mm;<br>Overlap 40 mm,<br>Groove-on top face of the bottom plate | CT, H13 tool steel; Shoulder: Ø 20 mm; Pin: conical, Ømax 7.5 mm, L 4.5 mm, angle 15 | CTFSLW;<br>No. of pass- 1, 2, 3<br>w 700 rpm; v 100 mm/min; Tool plunge 4.8 mm;<br>(SiC particles were added in the groove) | 1 pass resulted poor mixing; 3 passes resulted in proper mixing; 3 passes increased UTS up to 50% of reference conditions. | [35] |
| 15 | Al 6061 and AZ31Mg alloy (300 X 140 X 3) mm, Overlap 50 mm | CT;<br>External Shoulder: stationary;<br>Pin: includes an inner rotating tool | Dissimilar CTFSLW;<br>w 1000 rpm; v 20 mm/min | Small flash formation by the application of a stationary Shoulder also resulted in a smooth surface; Al12Mg17 IMC and Al3Mg2 IMC formed in the Al/Mg joint and Mg/Al joint, respectively at the boundary of NZ; Increased welding distance produced tunnel defect in the Al/Mg joint; TSF load of the Al/Mg joints was much smaller than that of the Mg/Al joints. | [7] |
| 16 | Al 6022, T 1 mm;<br>low carbon electro galvanized steel alloy, T 0.7 mm | CT, H13 tool steel, scribe insert- Tungsten carbide in a cobalt matrix;<br>Shoulder: flat, Ø 0.365";<br>Pin: cylindrical, Ø 0.158", L 0.036"; | Dissimilar CTFSLW with Scribe;<br>v (20-30) ipm; Offset distance 0.045" | The scribe tool is useful for FSLW Al and steel; Weld produced with the largest scribe tool resulted in TFL 3.6 kN; Lower v produced weld with higher TFL; Weld strength was affected by hook shape and size, as a dull and small hook could cover over a larger surface resulted in positive strength. | [36] |

| | | | | | |
|---|---|---|---|---|---|
| | | Scribe: different scribe geometries Ø 0.059”, L 0.010” | | | |
| 17 | AZ31B Mg and 7075-T6 Al dissimilar alloys (200 X 100 X 3) mm | CT; Shoulders: Ø 13 mm, concentric-circle-flute; Pin: Ømax 6 mm, Ømin 4 mm, L 4 mm, right-screwed pin | Dissimilar CTFSLW, w (600-800-1000-1200) rpm; v 50 mm/min; Tool tilt 2.5°; Plunge depth of the rotating tool shoulder 0.15 mm | Higher EST, ELW, NZ due to use of Zn as an interlayer; TFL was improved due to formation of dispersed Mg-Zn IMC as continues Mg-Zn IMC reduces TFL; At w 1000 rpm, maximum TFL reached at 6.6 K N with Zn interlayer. | [37] |
| 18 | Top plate- Al 2024 (200 X 100 X 2) mm; Bottom plate- Al 2024 (200 X 100 X 3) mm; Overlap 50 mm. | CT, H13 tool steel (hot worked); Shoulder: Ømax 15 mm, Ømin 6.1 mm; Pin: Ø 4.1 mm, L 3 mm, cylindrical RH threaded | CTFSLW; w 1000 rpm; v (100, 150, 200) mm/min | EST of top plate increase on AS and RS as w increases; and gap between two alclads (wave-shaped) decreases; During tool plunging, interface bending on AS and RS was found symmetric; During welding, bigger interface bending was found on AS than that on RS; Higher peak interface temperature was found on AS near weld bottom; Gradually increment in equivalent plastic strain was observed with the distance decrement to the weld centre. | [38] |
| 19 | Al 7075-T6 and AZ31B; Top Plate- Mg alloys (200 X 150 X 3) mm; Pure Zn foil as an interlayer, (200 X 150 X 0.1) mm | CT; Shoulder: Ø 14 mm, concentric-circle-flute; Pin: Ømax 5.6 mm, Ømin 3.8 mm, L 3.65 mm, right-screwed | CTFSLW; w 1000 rpm; v 50 mm/min; Tool tilting 2.5º; Plunge depth 0.15 mm; Ultrasound assisted (ultrasound vibration frequency 20 kHz, output power 1200 W) | ELW increased with ultrasound-assisted FSLW with Zn; Interlocking (Mechanical) improved, and formation of dispersed and finer Mg-Zn IMC; UTS max reached at 268 N/mm. | [39] |
| 20 | Galvanized low carbon steel plates, T 1 mm; Overlap 40 mm | CT, Tungsten carbide; Shoulder: Ø (10, 12, 14, 16) mm, concentric-circle-flute; Pin: pinless | CTFSLW, TAFW; w (600-800-1200-1400) rpm; v (200-400-600-800-1000-1200) mm/min; Tool tilting 2.5º; Tool plunge 0.5 mm | In most of the welds, important defects disappeared or as no string material; In weld morphology, a sound asymmetry was reported in the welds at higher w and v (due to the sticking to sliding characteristic). | [40] |
| 21 | AA1100 (80X 80 X 2) mm | CT, 13 tool steel (hot worked); Shoulder: Ø 16 mm, Flat; Pin: square, pentagon, hexagon, circle Ø 2.5 mm, L 3 mm | CTFSLW; w (400-800-1250-1600) rpm; v (20, 50, 80, 125) mm/min; Tool tilting (1º, 2º, 3º, 4º) | Adequate flow of material produced due to the generated maximum temperature (374 ºC); Increased w/v resulted in a higher amount of heat generation; Higher amount of heat generation and lower tool force was observed with the application of the tool profile of pentagon and square shape due to heavily localized plastic deformations in workpieces. | [41] |
| 22 | AA6082-T6 (heat treatable) AA5754-H22 (non-heat treatable) | CT, H13 tool steel; Pin: conical, Ømax 8 mm, Ømin 4 mm | CTFSLW; w (350-700-1200) rpm; v (350) mm/min, Tool tilting 2º; Tool plunge 1.2 mm. | Non-heat treatable alloy was less sensitive to the formation of weld defects than the heat treatable alloy; A sound asymmetry in weld properties was reported on AS and RS of the heat treatable alloy due to higher welding defect formation; TSL was independent to ELW (in between the two plates); TSL was depend on the formed defects on AS and RS. | [42] |

In order to reduce flaws and enhance joint quality in friction stir-welded butt and lapped workpieces, several traditional/conventional FSW tools and shapes, particularly those of pins, have been documented in the literature [43-45]. Detailed literature review on CTFSLW, CTFSBW and BTFSLW are summarised in Table 1. Very little research has been done on BTFSLW of Aluminum alloys [5, 12]. Very few or null literature was found on the BTFSLW of Al 6061-T6 workpieces. Weld formation in FSW is a very intricate process involving dynamic thermo-mechanical and metallurgical actions of the tool. Investigations with the novel tool is needed to generate effective horizontal as well as vertical flow of workpiece material and address a significant challenge in material flow towards the faying surface and intermixing of workpiece material at the weld interface in the lap configuration. In the present paper, such challenges are addressed with a novel tool, and the mechanical and macrostructure characteristics of FGBTFSLW are identified.

## 2. Materials and Methods

As a workpiece material, 3 mm thick rolled Aluminum alloy 6061-T6 plates with dimensions of 152 mm long by 102 mm wide was used for investigation. Workpiece material properties (Mechanical) and composition in wt. % (chemical) of Parent Metal (BM) is shown in Table 2.

Fixed gap bobbin tool friction stir lap welding (FGBTFSLW) was performed in an overlap dimension of 152 mm length and 72 mm width, as shown in Figure 3.

FSW in lapped configuration was performed at 90° to the plate rolling direction and along the plate length. Oxide layers on the top and bottom surfaces of the workpieces are removed with light rubbing and special chemicals to overcome the defect of ROD.

**Table 2. Workpiece material properties (Mechanical) and Composition wt. % (Chemical)**

| Properties (Mechanical) | | | Composition wt. % (Chemical) | | | | | | | |
|---|---|---|---|---|---|---|---|---|---|---|
| UTS (MPa) | Elongation (%) | Hardness (HV) | Mg | Fe | Si | Cr | Cu | Mn | Zn | Al |
| 282 | 21 | 80-90 | 0.937 | 0.553 | 0.457 | 0.266 | 0.173 | 0.106 | 0.01 | Bal |

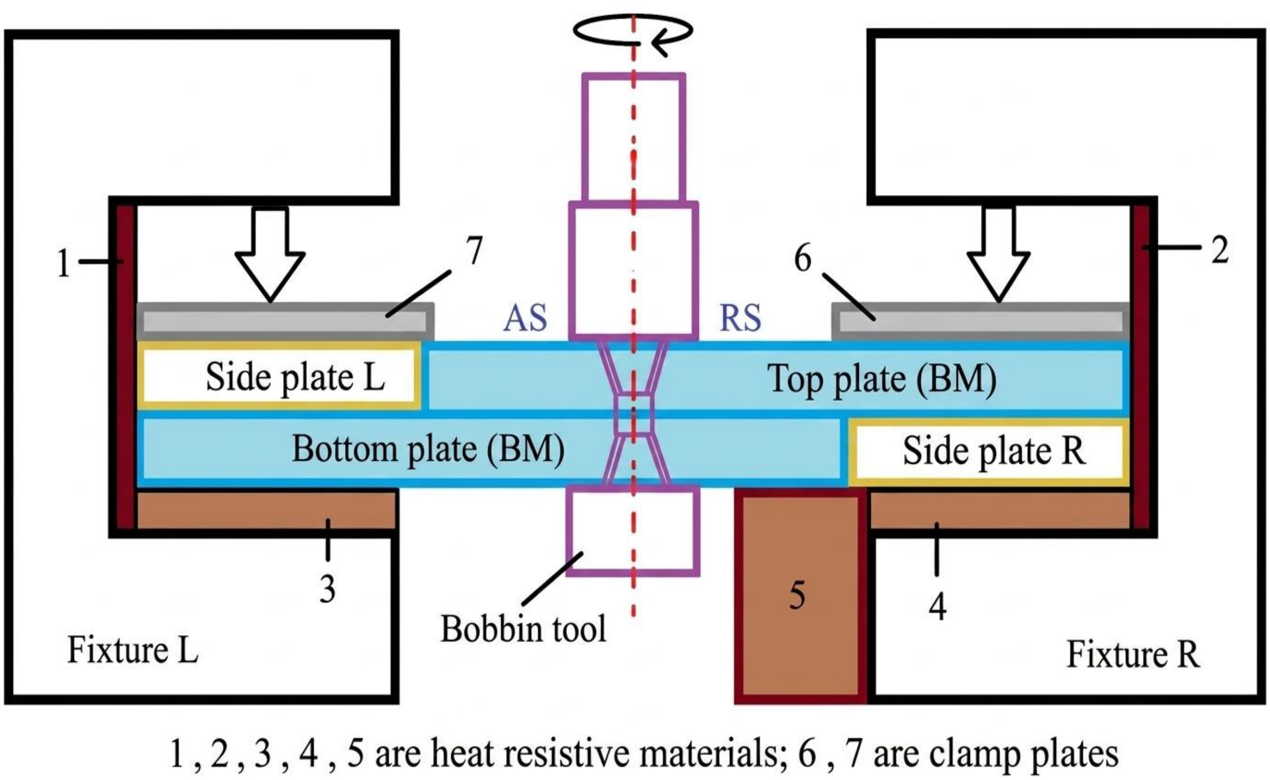


**Fig. 5 Schematic of experiment layout**

**Table 3. Bobbin tool dimensions and features**

| Upper Shoulder | | | | Pin | | | | | | Lower Shoulder | | | | Notes |
|---|---|---|---|---|---|---|---|---|---|---|---|---|---|---|
| Diameter [USD] (mm) | Length [TSL] (mm) | Primary Feature [USPF] | Secondary Feature [USSF] | Diameter [DP] (mm) | Largest [LDP] (mm) | Smallest [SDP] (mm) | Length [PL] (mm) | Primary Feature [PPF] | Secondary Feature [PSF] | Diameter [LSD] (mm) | Length [LSL] (mm) | Primary Feature [LSPF] | Secondary Feature [LSSF] | |
| 24 | 20 | Cylindrical | 2° Concave | 8 | 10 | 8 | 5.88 | Opposite frustum with cylindrical connect | LH thread, 3 flutes, RH thread | 24 | 12 | Cylindrical | 2° Concave | VIJNIS tool |

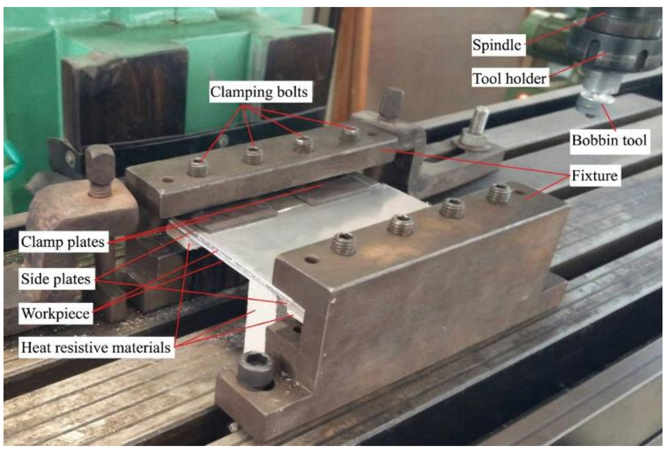


**Fig. 6 Experimental setup**

A special fixture was used for FGBTFSLW, which is shown in Figure 4. Holding areas of both plates were covered with heat-resistant materials to perform experiments in conductive heat flow restriction mode, as visible in Figure 5 and Figure 6. Figure 6 shows the experiment setup for FGBTFSLW. A heavy build vertical milling machine (machine-Sigma model, Geeta machine tools) was used for all the experiments.

A newly designed patented fixed gap bobbin tool for lapped workpieces [46], with 3 different profile parts in a pin and concave shoulders, was used for investigation, as shown in Figure 7 (a)-(c). Novel bobbin tool dimensions, and primary and secondary features of the tool pin and both the shoulders are shown in Table 3. Diameters of both (top and bottom) shoulders were designed to be 24 mm, and a concave feature was used on both the Shoulder surfaces towards the pin.

The tool pin was designed with unique, three distinct profile parts to stir the material horizontally and vertically towards mating surfaces. Upper and lower parts were opposite frustum with helical threads, a maximum diameter of 10 mm at the shoulder side and a minimum diameter of 8 mm at the cylindrical mid part of the pin. LH threads were made on the top part of the pin, and RH threads were made on the bottom part of the pin with the same helix angle.

Three flutes were made on the cylindrical mid part of the pin. Such features were designed on a pin that generates material flow horizontally and dynamic intermixing of top plate and bottom plate material flow directed vertically towards mating surfaces by rotating the upper pin and lower pin parts, as it is the most critical requirement for good quality friction stir welding in a lap configuration.

A different set of combinations of tool feeds and tool rotational speeds were applied initially in a number of trials. Based on visual observations of initial welded samples, the operating window for welding speed and rotational speed was decided. Three different rotation speeds- 280, 350 and 445 RPM and a fixed tool feed of 16 mm/min were used to investigate effects on Mechanical properties and micro structure in FGBTFSLW.

The samples were cut in the transverse direction of the weld specimen with the help of wire EDM after FGBTFSLW for the study of metallographic and load-bearing capacity in tensile-shear. From each weldment, 3 samples for tensile-shear testing and one sample for metallographic study for each weld specimen.

The average tensile-shear strength value of three samples used for tensile-shear testing was appropriate for the results. Samples were cut, polished and prepared for metallographic study using Keller’s reagent. An optical microscope (Olympus GX51, Tokyo, Japan) was used for metallographic examinations. Vickers microhardness indentation machine (Omnitech MVH-S-Auto, Metatech, Pune) was used for microhardness measurements on polished cross-sections having a 0.5 mm interval. A 300 gm. load was applied with a 10 seconds dwell time during the measurement.

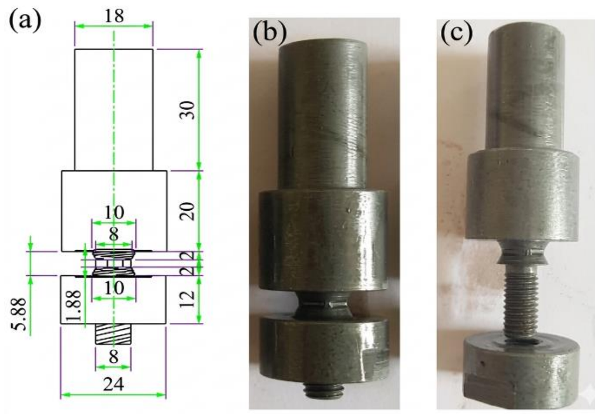


**Fig. 7 Tool used in experiment (a) 2D drawing, (b) Assembled, (c) Disassembled.**

The tensile-shear test specimens were prepared in accordance with the AWS D17.3/D17.3M:2016 standard. The average tensile strength was determined from 3 specimens' tests. Tensile tests were carried out at room temperature using a computer-controlled universal testing machine (M-100 model/FSA) with a crosshead speed (1 mm/min), as shown in Figure 13.

## 3. Results and Discussion

In the present paper, an experiment was performed with the conductive heat restriction flow mode with the shielding of both workpieces by heat restrictive material, as shown in Figure 6. By applying this heat-restrictive mode to workpieces, loss of frictional heat due to conductive heat flow towards fixtures and towards the machine tool, ultimately, is reduced, which will reduce the requirement of high rotational speed of the tool. Control of heat restrictions and rotational speed of tool and feed produce sufficient frictional heat, and plasticized material must needed in FSW. An air cooling approach was used for the weld specimens in the experiment.

### *3.1. Weld Formation*

As shown in Figure 8 (a)-(f), the weld surface morphology of the top and bottom plates shows a smooth surface with fine shoulder marks. Entry holes and exit holes with a tail are visible as a characteristic of BTFSW. Defect-free lap joints were observed with little flash generated at the retrieving side shows adequate shoulder gap. Visible groove marks were observed at the advancing side. Very less material sticking was observed on the bobbin tool. The surface morphology study proves an adequate gap in between the bobbin tool shoulders (0.98 % of the lap thickness of workpieces). Appropriate interaction among the bobbin tool and workpieces is needed for sufficient heat generation and dynamic intermixing of workpiece materials for a quality lap weld.

### *3.2. Macrostructure Characteristics*

Figure 9 (a-c) shows the macrostructures of FGBTFSLW with four microstructure zones and separated by virtual lines. As a characteristic of BTFSW, an hourglass-shaped Nugget Zone (NZ) or Weld Nugget Zone (WNZ) is visible in all the samples and again separated in three zones – Nugget Zone Top (NZT), Nugget Zone Middle (NZM), and Nugget Zone Bottom (NZB), indicated in the top, middle and bottom sections, respectively. TP represents the top plate, whereas BP represents the bottom plate. The hourglass shape is clearly visible on AS but difficult to separate on RS due to the centrifugal forging of material with the base material. The band pattern is also visible in the WNZ or NZ. TMAZ, HAZ, and BM are next to NZ in order, respectively. As shown in Figure 9 (a), the welding defect, as two voids at AS in NZM, for the experiment with a tool rotation speed of 280 RPM, indicates insufficient heat generation due to lower friction heat and poor intermixing due to insufficient dynamic rotational force due to a low rotational speed of the tool compared to the required one. No identification of a separate weld region observed towards RS indicates sufficient intermixing of materials towards RS. Horizontal interface line in between top and bottom workpiece material is shifted towards the downward side near the NZ, shows downward hooking, whereas on RS common interface line is shifted towards the upward side shows upward cold lap. Hooking and cold lap characteristics [22], in FSLW are highly responsible for stress propagator during tensile-shear testing and reduce the tensile-shear strength of FSLW.

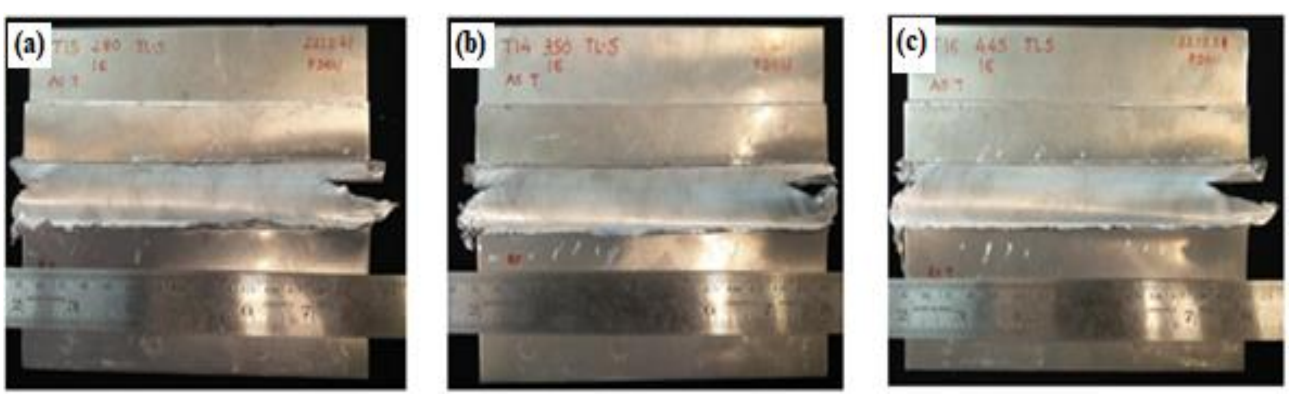

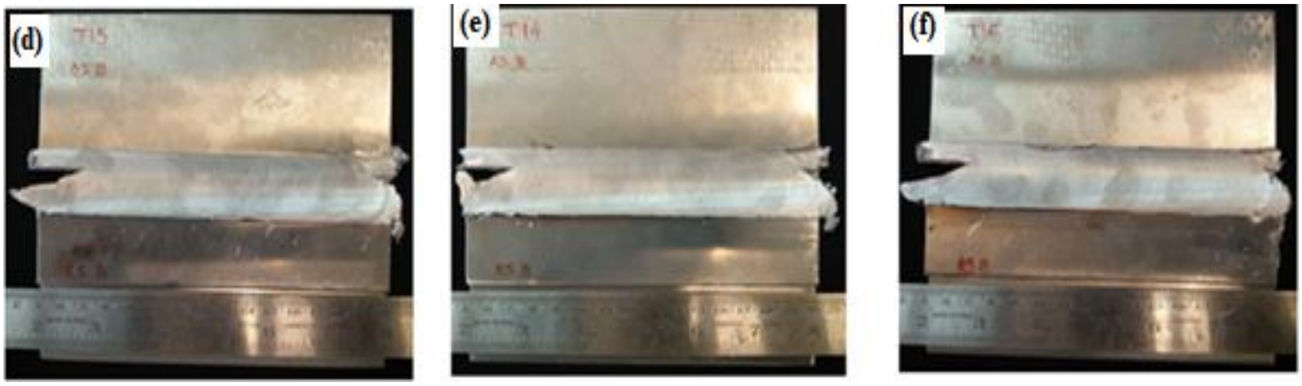


**Fig. 8 Weld surface morphology of specimens: Top view, (a) Spindle speed- 280 RPM, (b) Spindle speed- 350 RPM, (c) Spindle speed- 445 RPM Bottom view- (d) spindle speed- 280 RPM, (e) spindle speed- 350 RPM, (f) spindle speed- 445 RPM.**

As shown in Figure 9 (b), a welding defect as a single void at AS in NZM for the experiment with a tool rotation speed of 350 RPM indicates still poor intermixing due to insufficient dynamic rotational force than the required one for sufficient intermixing of materials. Different regions of the weld specimen are visible in Figure 9 (b), which indicates a little change in the shape of NZ. Downward hook and upward cold lap are also shown in Figure 9 (b).

No welding defect or void are observed at any portion of NZ as shown in Figure 9 (c) for the experiment with tool rotation speed of 445 RPM, which indicates sufficient intermixing of workpiece materials due to requires dynamic rotational force. The downward shifting effect is also reduced in the hook, whereas upward lifting is reduced in the cold lap, which reduces plate thinning and thickening effect and resulted in improved tensile-shear strength of the weld specimen.

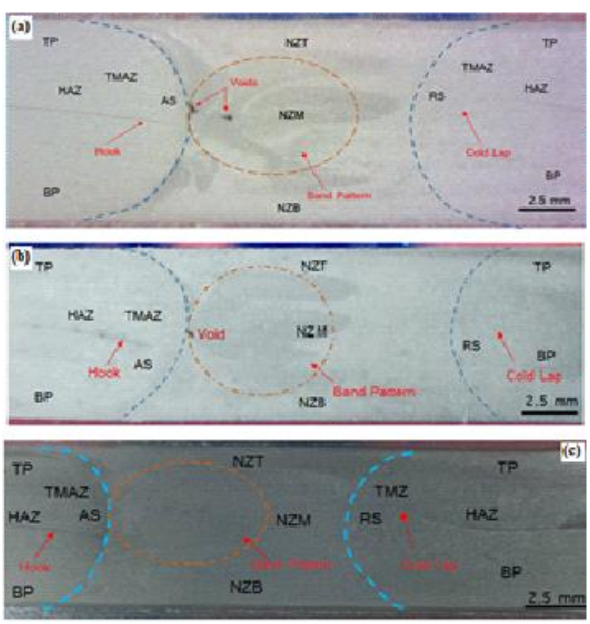


**Fig. 9 Macrographs of BTFSW joints with 16 mm feed for the different rotational speeds, (a) Speed-280 RPM, (b) Speed-350 RPM, (c) Speed-445 RPM.**

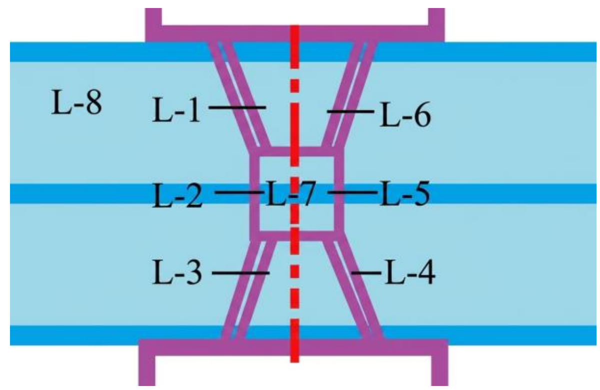


**Fig. 10 Microstructure locations and notations**

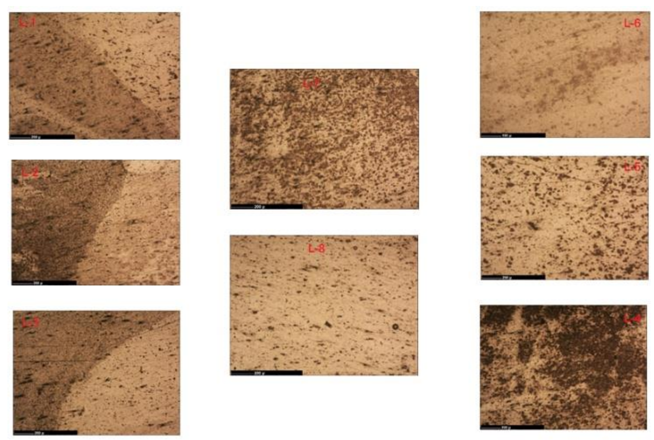

**Fig. 11 Microstructure of weld specimen with speed 445 RPM, feed 16 mm**

### *3.3. Microstructural Characteristics*

As shown in Figure 10, microstructures for all weld specimens were investigated for eight locations as L.1, L.2, L.3, L.4, L.5, L.6, L.7 and L.8 used as indicators for lap weld at AS on TP, AS centre line, AS on BP, RS on TP, RS centre line, RS on BT, vertical middle line of NZ and BM of top pale respectively. Figure 11 illustrates the representative microstructures observed in the various zones of the FGBTFSLW joint fabricated at a tool rotation speed of 445 rpm and a tool feed of 16 mm/min. Elongated course gain observed in the BM as shown in Figure 11 L.8. As compared to the BM, the HAZ shows uniform grain size distribution due to the effect of thermal cycling only, shown in shown in Figure 11 L.1, L.3, L.6 and L.6. Figure 11 L.2 indicates the interface of the workpieces' mating surface at the WNZ. Grains are elongated due to the rotational force of the tool in the TMAZ region. Some equiaxed and fine grains were formed because of little material re-crystallization in TMAZ. Figure 11 L.7 shows uniformly distributed fine equiaxed fine grains due to a large amount of plastic deformation and flow material forging produced by the bobbin tool.

### *3.4. Tensile Properties*

The top views of tensile-shear tested specimens are visible in Figure 12 (a)-(c) for with rotational speed of 280 RPM, 350 RPM and 345 RPM. Figure 12 (d)-(f) show side views of tensile-shear tested specimens with rotational speeds of 280 RPM, 350 RPM and 345 RPM. All weld samples were fractured in tensile failure only; no shear failure was not observed in any sample, which indicates very strong lap joint welding with the newly designed bobbin tool. All weld samples were fractured from advancing side of bottom plate in tensile-shear test.

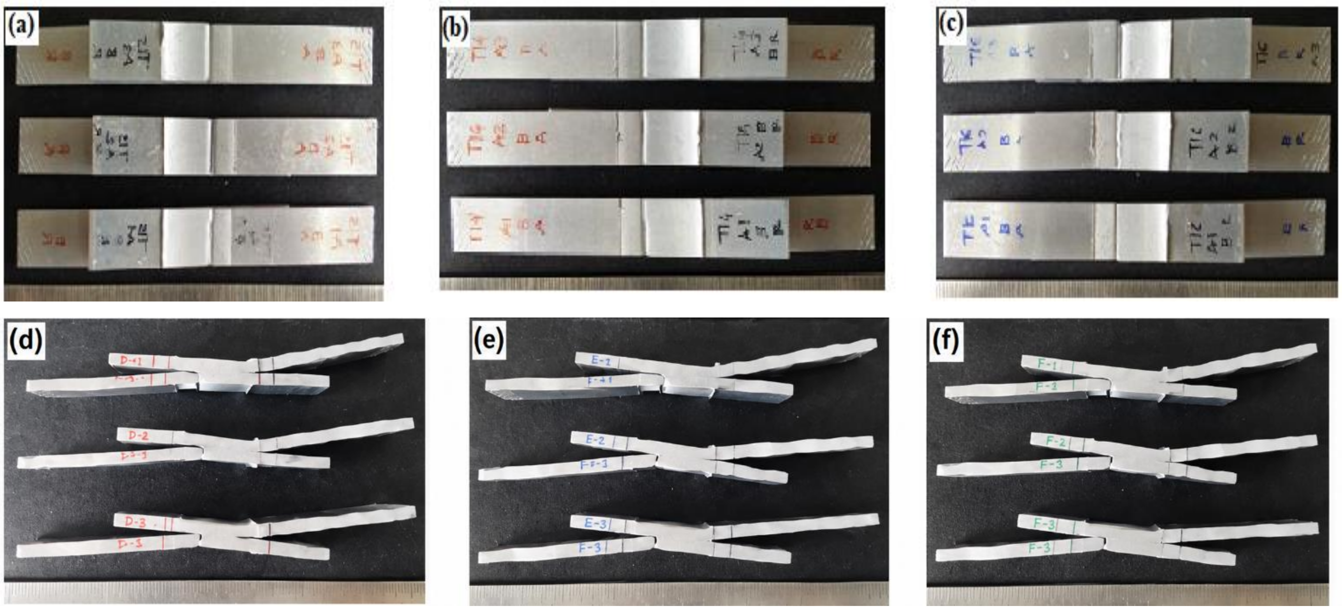


**Fig. 12 Tensile-shear fracture in specimens: top views- (a) Spindle speed- 280 RPM, (b) Spindle speed- 350 RPM, (c) Spindle speed- 445 RPM, side views- (d) Spindle speed- 280 RPM, (e) Spindle speed- 350 RPM, (f) Spindle speed- 445 RP.**

**Fig. 13 Tensile-shear testing of specimen on universal testing machine M-100, FSA**

**Table 4. Tensile-shear test result (feed rate-16 mm/min)**

| RPM | UTS (N/mm$^2$) | Elongation (%) |
|---|---|---|
| 280 | 109.00 | 3.31 |
| 350 | 114.37 | 2.39 |
| 445 | 136.98 | 4.45 |

The tensile properties are shown in Table 4 and represented in Figure 14. The tensile strength of the weld specimen is 109.00 N/mm$^2$, 114.37 N/mm$^2$ and 136.98 N/mm$^2$ for tool rotational speeds of 280 RPM, 350 RPM and 445 RPM, respectively. Elongation % is 3.31, 2.39 and 4.45 for tool rotational speeds of 280 RPM, 350 RPM and 445 RPM, respectively. The maximum tensile-shear strength value of 136.98 N/ mm$^2$ is achieved for a tool rotational speed of 445 RPM. This can be attributed to the forged effect of tool shape with sufficient material flow conditions. The results indicate that the weld produced using 445 rpm tool rotation speed and 16 mm/min tool feed demonstrated marginally improved strength due to the uniform cooling rate and controlled thermal distribution associated with the tool geometry.

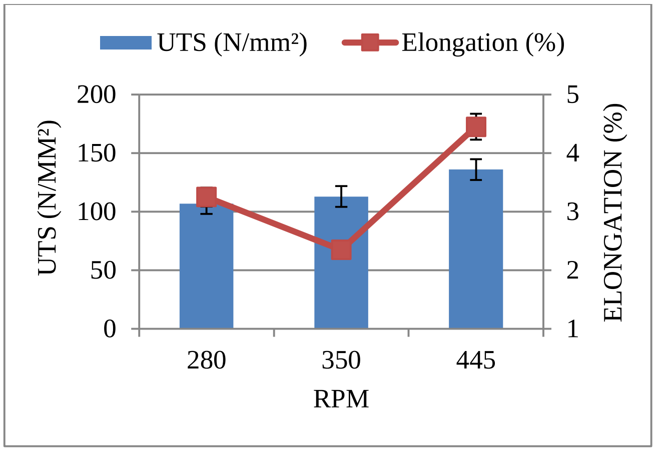


**Fig. 14 Tensile-shear failure**

### *3.5. Microhardness Properties*

Figure 15 presents the microhardness profiles of all three specimens measured along the centreline of the cross-sectional surface (in thickness direction). For each specimen, microhardness values were measured from various points of the upper part of the top plate, lower part of the bottom plate and the mid part of the weld sections with reference to specific distances from the vertical centreline of the weld along the thickness and averaged with respect to specific distances from the vertical centreline of the weld.

With respect to Figure 15, we can conclude that all the samples show symmetrical microhardness distribution like a shallow W-shaped profile. The weld specimen with a tool rotational speed of 445 RPM reported a higher hardness value at TMAZ adjacent to NZ. HAZ shows lower hardness compare to all zones.

Figure 16 shows the average microhardness value for the top plate, and Figure 17 shows the average microhardness value for the bottom plate for all three weld specimens. Both graphs indicate that the microhardness average value is identical in the top and bottom plates in welding with a threaded pin profile.

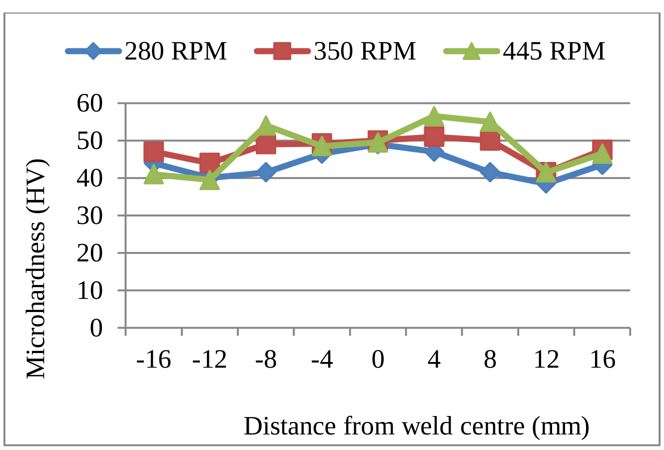


**Fig. 15 Average microhardness**

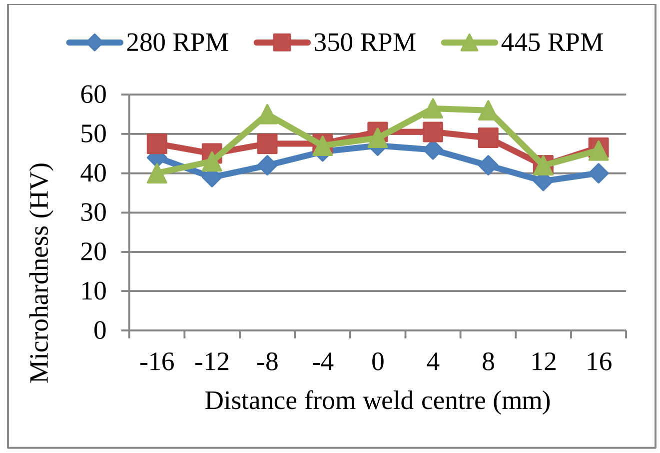


**Fig. 16 Average microhardness of the top plate**

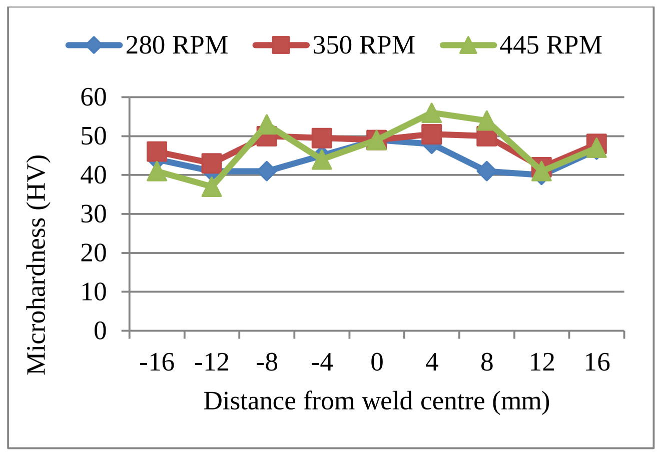


**Fig. 17 Average microhardness of the bottom plate**

## 4. Conclusion

In the research article, the results of the investigation of the experiment performed with the fixed tool feed rate 16 mm/min; 3 different tool rotation speeds: 280 RPM, 350 RPM and 445 RPM (as operating parameters) and novel designed bobbin tool for lapped configuration (as tool parameters) used for FGBTFWLW of Al 6061-T6 plates having thickness of 3 mm to reveal microstructure and mechanical properties. Research conclusions are as follows.

1) Very good lap weld quality was achieved at a lower welding speed in the newly designed bobbin tool.
2) Bobbin tool with LH and RH threaded pin resulted very good quality lap weld.
3) Very good quality FGBTFSL welds were achieved at a tool rotational speed of 445 RPM, feed rate of 16 mm, with a threaded bobbin tool.
4) Low tool rotational speed (RPM) needed due to heat flow restriction applied in the experiment setup.
5) Weld joint quality and strength was increased with an increment in tool rotation speed from 280 to 445 RPM
6) All weld samples were fractured in tensile failure only. Shear failure was not observed in any sample, which

indicates very strong lap joint welding with the newly designed bobbin tool.

7) All weld samples were fractured from advancing side of bottom plate in the tensile-shear test.
8) The maximum ultimate tensile strength (UTS) value 136.98 N/mm$^2$ was observed at a tool rotational speed of 445 RPM, feed rate 16 mm, with a threaded pin bobbin tool in tensile testing.
9) The maximum ultimate tensile strength (UTS) value was 48.57% compared to the UTS of the base material, N/mm$^2$, which was observed at a tool rotational speed of 445 RPM, feed rate 16 mm, with a threaded pin bobbin tool in tensile-shear testing.
10) Maximum micro hardness value 56.6 Hv was observed at tool rotational speed 445 RPM, feed rate 16 mm, with threaded pin profile.
11) The microhardness value was higher at TMAZ and lower at HAZ.
12) Microhardness value increased with increased tool rotational speed. 9.07% upside micro hardness value was observed at a tool rotation speed of 445 RPM compared to a tool rotational speed of 280 RPM.
13) The microhardness average value was identical in the top and bottom plates in welding with a threaded pin profile.
14) Microhardness average value was 2.9% higher on RS compared to AS in welding with a threaded pin profile.

## Conflicts of Interest

The authors attest to having no conflicts of interest.

## Funding Statement

The authors did not receive any external grants or sponsorships for this investigation.

## Acknowledgments

The authors gratefully acknowledge Pandit Deendayal Energy University (PDEU), Gandhinagar, Gujarat, India, for providing the essential infrastructure, equipment, and support required to conduct this research. FSLWs were performed on heavy built vertical milling machine, Sigma, Geeta Machine Tools and weld samples were cut on wire EDM facilitated by the Machining center, Department of Mechanical Engineering, PDEU, Gandhinagar.

## References

[1] L. Dubourg, A. Merati, and M. Jahazi, "Process Optimisation and Mechanical Properties of Friction Stir Lap Welds of 7075-T6 Stringers on 2024-T3 Skin," *Materials & Design*, vol. 31, no. 7, pp. 3324-3330, 2010. [CrossRef] [Google Scholar] [Publisher Link]

[2] Wayne M. Thomas et al., "Friction Stir Welding," *U.S. Patent US5460317A*, pp. 1-19, 1991. [Google Scholar] [Publisher Link]

[3] Nitin Panaskar, and Ravi Terkar, "A Review on Recent Advances in Friction Stir Lap Welding of Aluminium and Copper," *Materials Today: Proceedings*, vol. 4, no. 8, pp. 8387-8393, 2017. [CrossRef] [Google Scholar] [Publisher Link]

[4] Seung Hwan C. Park et al., "Rapid Formation of the Sigma Phase in 304 Stainless Steel During Friction Stir Welding," *Scripta Materialia*, vol. 49, no. 12, pp. 1175-1180, 2003. [CrossRef] [Google Scholar] [Publisher Link]

[5] Sattar S. Emamian et al., "Improving the Friction Stir Welding Tool Life for Joining the Metal Matrix Composites," *The International Journal of Advanced Manufacturing Technology*, vol. 106, no. 7, pp. 3217-3227, 2020. [CrossRef] [Google Scholar] [Publisher Link]

[6] C. Yang et al., "A Comparative Research on Bobbin Tool and Conventional Friction Stir Welding of Al-Mg-Si Alloy Plates," *Materials Characterization*, vol. 145, pp. 20-28, 2018. [CrossRef] [Google Scholar] [Publisher Link]

[7] Shude Ji et al., "Effect of Lap Configuration on Magnesium to Aluminum Friction Stir Lap Welding Assisted by External Stationary Shoulder," *Materials & Design*, vol. 103, pp. 160-170, 2016. [CrossRef] [Google Scholar] [Publisher Link]

[8] Bo Li et al., "Effects of Processing Variables and Heat Treatments on Al/Ti-6Al-4V Interface Microstructure of Bimetal Clad-Plate Fabricated via a Novel Route Employing Friction Stir Lap Welding," *Journal of Alloys and Compounds*, vol. 658, pp. 904-913, 2016. [CrossRef] [Google Scholar] [Publisher Link]

[9] Yanxin Zhang et al., "Friction Stir Lap Welding of AA2024-T4 with Drastically Different Thickness," *The International Journal of Advanced Manufacturing Technology*, vol. 106, no. 9, pp. 3683-3691, 2020. [CrossRef] [Google Scholar] [Publisher Link]

[10] Y.C. Chen, and K. Nakata, "Microstructural Characterization and Mechanical Properties in Friction Stir Welding of Aluminum and Titanium Dissimilar Alloys," *Materials & Design*, vol. 30, no. 3, pp. 469-474, 2009. [CrossRef] [Google Scholar] [Publisher Link]

[11] R.S. Mishra, and Z.Y. Ma, "Friction Stir Welding and Processing," *Materials Science and Engineering: R: Reports*, vol. 50, no. 1-2, pp. 1-78, 2005. [CrossRef] [Google Scholar] [Publisher Link]

[12] Abhishek Sharma et al., "Friction Stir Lap Welding of AA6061 Aluminium Alloy with a Graphene Interlayer," *Materials*, vol. 35, no. 3, pp. 258-269, 2020. [CrossRef] [Google Scholar] [Publisher Link]

[13] Omar S. Salih et al., "Microstructure and Mechanical Properties of Friction Stir Welded AA6092/SiC Metal Matrix Composite," *Materials Science and Engineering: A*, vol. 742, pp. 78-88, 2019. [CrossRef] [Google Scholar] [Publisher Link]

[14] Dario Baffari et al., "Experimental and Numerical Investigation on a New FSW Based Metal to Composite Joining Technique," *Journal of Manufacturing Processes*, vol. 34, pp. 758-764, 2018. [CrossRef] [Google Scholar] [Publisher Link]

[15] P.S. De, and R.S. Mishra, "Friction Stir Welding of Precipitation Strengthened Aluminium Alloys: Scope and Challenges," *Science and Technology of Welding and Joining*, vol. 16, no. 4, pp. 343-347, 2011. [CrossRef] [Google Scholar] [Publisher Link]

[16] R. Rai et al., "Review: Friction Stir Welding Tools," *Science and Technology of Welding and Joining*, vol. 16, no. 4, pp. 325-342, 2011. [CrossRef] [Google Scholar] [Publisher Link]

[17] Philip L. Threadgill et al., "The Use of Bobbin Tools for Friction Stir Welding of Aluminium Alloys," *Materials Science Forum*, vol. 638-642, pp. 1179-1184, 2010. [CrossRef] [Google Scholar] [Publisher Link]

[18] Milan Pecanac et al., "Influence of Tool and Welding Parameters on the Risk of Wormhole Defect in Aluminum Magnesium Alloy Welded by Bobbin Tool FSW," *Metals*, vol. 12, no. 6, pp. 1-14, 2022. [CrossRef] [Google Scholar] [Publisher Link]

[19] G. Buffa et al., "Friction Stir Welding of Lap Joints: Influence of Process Parameters on the Metallurgical and Mechanical Properties," *Materials Science and Engineering: A*, vol. 519, no. 1-2, pp. 19-26, 2009. [CrossRef] [Google Scholar] [Publisher Link]

[20] Rathinasuriyan Chandran et al., "Optimization of Welding Parameters for Friction Stir Lap Welding of AA6061-T6 Alloy," *Modern Mechanical Engineering*, vol. 8, no. 1, pp. 31-41, 2018. [CrossRef] [Google Scholar] [Publisher Link]

[21] Tanmoy Medhi et al., "Multi-Pass Friction Stir Lap Welding of AA 6061-T6: Implication of Tool Pin Overlapping on Microstructure and Mechanical Properties of Joints," *Welding & Inspection*, vol. 27, 2022. [CrossRef] [Google Scholar] [Publisher Link]

[22] Xiaodong Xu et al., "Microstructures and Fatigue Properties of Friction Stir Lap Welds in Aluminum Alloy AA6061-T6," *Materials & Design*, vol. 35, pp. 175-183, 2012. [CrossRef] [Google Scholar] [Publisher Link]

[23] Simon Larose, Maxime Guérin, and Priti Wanjara, "Process Window for Friction Stir Lap Welding of Aluminum Alloy 6061," *Materials Science Forum*, vol. 783-786, pp. 2839-2844, 2014. [CrossRef] [Google Scholar] [Publisher Link]

[24] Antonello Astarita et al., "Dissimilar Friction Stir Lap Welding of AA2198 and AA7075 Sheets: Forces, Microstructure and Mechanical Properties," *The International Journal of Advanced Manufacturing Technology*, vol. 117, no. 3, pp. 1045-1059, 2021. [CrossRef] [Google Scholar] [Publisher Link]

[25] Vijaykumar Natvarlal Modi et al., "Weld Formation Investigations of FSW of Al 6061-T6 Lapped Workpieces Using Dual Shoulders Tool," *International Journal of Research and Innovation in Applied Science*, vol. 11, no. 6, pp. 623-642, 2026. [CrossRef] [Google Scholar] [Publisher Link]

[26] Mohamed M.Z. Ahmed et al., "Bobbin Tool Friction Stir Welding of Aluminum: Parameters Optimization Using Taguchi Experimental Design," *Materials*, vol. 15, no. 8, pp. 1-18, 2022. [CrossRef] [Google Scholar] [Publisher Link]

[27] Mohamed M. Z. Ahmed et al., "Bobbin Tool Friction Stir Welding of Aluminum Thick Lap Joints: Effect of Process Parameters on Temperature Distribution and Joints' Properties," *Materials*, vol. 14, no. 16, pp. 1-22, 2021. [CrossRef] [Google Scholar] [Publisher Link]

[28] Yazid Helal, Zakaria Boumerzoug, and Lahcene Fellah, "Microstructural Evolution and Mechanical Properties of Dissimilar Friction Stir Lap Welding Aluminum Alloy 6061-T6 to Ultra-Low Carbon Steel," *Energy Procedia*, vol. 157, pp. 208-215, 2019. [CrossRef] [Google Scholar] [Publisher Link]

[29] Mingrun Yu et al., "Microstructure and Mechanical Properties of Friction Stir Lap AA6061-Ti6Al4V Welds," *Journal of Materials Processing Technology*, vol. 270, pp. 274-284, 2019. [CrossRef] [Google Scholar] [Publisher Link]

[30] Yang Zhou et al., "Influences of Pin Shape on a High Rotation Speed Friction Stir Welding Joint of a 6061-T6 Aluminum Alloy Sheet," *Metals*, vol. 8, no. 12, pp. 1-13, 2018. [CrossRef] [Google Scholar] [Publisher Link]

[31] Zhenlu Zhou et al., "Effect of Rotating Speed on Joint Morphology and Lap Shear Properties of Stationary Shoulder Friction Stir Lap Welded 6061-T6 Aluminum Alloy," *The International Journal of Advanced Manufacturing Technology*, vol. 88, pp. 2135-2145, 2017. [CrossRef] [Google Scholar] [Publisher Link]

[32] Yongxian Huang et al., "Joining of Aluminum Alloy and Polymer Via Friction Stir Lap Welding," *Journal of Materials Processing Technology*, vol. 257, pp. 148-154, 2018. [CrossRef] [Google Scholar] [Publisher Link]

[33] G.R. Argade et al., "Friction Stir Lap Welding of Stainless Steel and Plain Carbon Steel to Enhance Corrosion Properties," *Journal of Materials Processing Technology*, vol. 259, pp. 259-269, 2018. [CrossRef] [Google Scholar] [Publisher Link]

[34] L.H. Wu, K. Nagatsuka, and K. Nakata, "Direct Joining of Oxygen-Free Copper and Carbon-Fiber-Reinforced Plastic by Friction Lap Joining," *Journal of Materials Science & Technology*, vol. 34, no. 1, pp. 192-197, 2018. [CrossRef] [Google Scholar] [Publisher Link]

[35] Gianluca Buffa, Davide Campanella, and Livan Fratini, "Enhancement of Mechanical Properties of FSWed AA7075 Lap Joints Through in-Situ Fabrication of MMC," *Journal of Manufacturing Processes*, vol. 28, no. 3, pp. 422-427, 2026. [CrossRef] [Google Scholar] [Publisher Link]

[36] Shiyu Niu et al., "AZ31B/7075-T6 Alloys Friction Stir Lap Welding with a Zinc Interlayer," *Journal of Materials Processing Technology*, vol. 263, pp. 82-90, 2019. [CrossRef] [Google Scholar] [Publisher Link]

[37] Q. Wen et al., "Experimental and Numerical Investigations of Bonding Interface Behavior in Stationary Shoulder Friction Stir Lap Welding," *Materials Science & Technology*, vol. 35, no. 1, pp. 192-200, 2019. [CrossRef] [Google Scholar] [Publisher Link]

[38] Shude Ji et al., "Friction Stir Lap Welding of Al to Mg Assisted by Ultrasound and a Zn Interlayer," *Journal of Materials Processing Technology*, vol. 267, pp. 141-151, 2019. [CrossRef] [Google Scholar] [Publisher Link]

[39] D.G. Andrade, C. Leitão, and D.M. Rodrigues, "Properties of Lap Welds in Low Carbon Galvanized Steel Produced by Tool Assisted Friction Welding," *Journal of Materials Processing Technology*, vol. 260, pp. 77-86, 2018. [CrossRef] [Google Scholar] [Publisher Link]

[40] Abolfazl Khalkhali, Salman Ebrahimi-Nejad, and Nima Geran Malek, "Comprehensive Optimization of Friction Stir Weld Parameters of Lap Joint AA1100 Plates using Artificial Neural Networks and modified NSGA-II," *Materials Research Express*, vol. 5, no. 6, 2018. [CrossRef] [Google Scholar] [Publisher Link]

[41] M. I. Costa, C. Leitao, and D. M. Rodrigues, "Influence of the Aluminium Alloy Type on Defects Formation in Friction Stir Lap Welding of Thin Sheets," *Welding & Inspection*, vol. 23, no. 1, pp. 32-42, 2018. [CrossRef] [Google Scholar] [Publisher Link]

[42] Mukesh Kumar, Ashish Das, and Raj Ballav, "Influence of Tool Geometry on Morphology and Mechanical Properties of Friction Stir Welded Dissimilar Joints: A Review," *Materials Today: Proceedings*, vol. 33, no. 8, pp. 4951-4955, 2020. [CrossRef] [Google Scholar] [Publisher Link]

[43] MohammadHosein Mirzaei, Parviz Asadi, and Ali Fazli, "Effect of Tool Pin Profile on Material Flow in Double Shoulder Friction Stir Welding of AZ91 Magnesium Alloy," *International Journal of Mechanical Sciences*, vol. 183, 2020. [CrossRef] [Google Scholar] [Publisher Link]

[44] R. Anand, and V. G. Sridhar, "Studies on Process Parameters and Tool Geometry Selecting Aspects of Friction Stir Welding – A Review," *Materials Today: Proceedings*, vol. 27, no. 1, pp. 576-583, 2020. [CrossRef] [Google Scholar] [Publisher Link]

[45] S. Rohani Yazdi, B. Beidokhti, and M. Haddad-Sabzevar, "Pinless Tool for FSSW of AA 6061-T6 Aluminum Alloy," *Journal of Materials Processing Technology*, vol. 267, pp. 44-51, 2019. [CrossRef] [Google Scholar] [Publisher Link]

[46] Firouz Fadaeifard et al., "Investigation of Microstructure and Mechanical Properties of Friction Stir Lap Welded AA6061-T6 in Various Welding Speeds," *Journal of Applied Sciences*, vol. 14, no. 3, pp. 221-228, 2014. [CrossRef] [Google Scholar] [Publisher Link]

## Appendix 1 (Abbreviations and full forms)

| Abbreviations | Full Term |
|---|---|
| CT | Conventional Tool |
| BT | Bobbin Tool |
| FSW | Friction Stir Welding |
| CTFSW | Conventional Tool Friction Stir Welding |
| FSLW | Friction Stir Lap Welding |
| BTFSW | Bobbin Tool Friction Stir Welding |
| CTFSBW | Conventional Tool Friction Stir Butt Welding |
| CTFSLW | Conventional Tool Friction Stir Lap Welding |
| BTFSLW | Bobbin Tool Friction Stir Lap Welding |
| FGBTFSLW | Fixed Gap Bobbin Tool Friction Stir Lap Welding |
| NZ | Nugget Zone |
| TMAZ | Thermo Mechanical Affected Zone |
| HAZ | Heat Affected Zone |
| BM | Base Material |
| BS | Base Plate |
| AS | Advancing Side |
| RS | Retreating Side |
| ROD | Residual Oxide Defect |
| w | Rotational Speed |
| v | Traveling Speed/Feed |
| Ø | Diameter |
| RH | Right Handed |
| LH | Left Handed |
| Tw | Temperature at Weld Centre |
| RPM | Revolution Per Minute |
| IPM | Inch Per Minute |
| UTS | Ultimate Tensile Strength |
| TSL | Tensile-Shear Load |
| TSF | Tensile-Shear Failure |
| EPT | Effective Plate Thickness |
| ELW | Effective Lap Width |
| SPW | Single Pass Welding |
| DPW | Double Pass Welding |
| EPT | Effective Plate Thickness |
| BPA | Bottom Plate Advancing side |
| TPA | Top Plate Advancing side |
| NZT | Nugget Zone Top Section |
| NZM | Nugget Zone of Middle Section |
| NZB | Nugget Zone Bottom Section |
| IMC | Inter Metallic Compound |